

## Induced Crystallization of Polyelectrolyte-Surfactant Complexes at the Gas-Water Interface

D. Vaknin,<sup>1</sup> S. Dahlke,<sup>1</sup> A. Travesset,<sup>1</sup> G. Nizri,<sup>2</sup> and S. Magdassi<sup>2</sup>

<sup>1</sup>Ames Laboratory and Department of Physics and Astronomy, Iowa State University, Ames, Iowa 50011, USA

<sup>2</sup>Institute of Applied Chemistry, Hebrew University of Jerusalem, Jerusalem, Israel 91904

(Received 12 January 2004; published 19 November 2004)

Synchrotron x-ray and surface-tension studies of a strong polyelectrolyte (PE) in the semidilute regime ( $\sim 0.1M$  monomer charges) with varying surfactant concentrations show that minute surfactant concentrations induce the formation of a PE-surfactant complex at the gas-solution interface. X-ray reflectivity and grazing angle x-ray diffraction show the complex PE-surfactant resides at the interface and the alkyl chains of the surfactant form a two-dimensional liquidlike monolayer. With the addition of salt (NaCl), columnar crystals with distorted-hexagonal symmetry are formed.

DOI: 10.1103/PhysRevLett.93.218302

PACS numbers: 82.70.Uv, 81.07.Nb, 82.35.Rs

There has been a growing interest in the phase behavior, aggregation, and precipitation of polymer-surfactant mixtures; in particular, ionic surfactants and oppositely charged flexible polyelectrolytes (PEs) [1–7], or semiflexible PEs, such as DNA [8] or actin [9]. In addition to the fundamental interest in the principles governing phase behavior, aggregation, and precipitation of polymer-surfactant mixtures, understanding the behavior of these complex systems is crucial for technological applications concerning detergents, paints, cosmetics, DNA transfection [10–12], and others.

Some important aspects regarding the formation of flexible polyelectrolyte-surfactant complexes present exciting challenges, both experimentally and theoretically. The role played by the interface in the growth and nucleation of these complexes, for example, is to a large extent unknown, although neutron and x-ray reflectivity studies provided invaluable insight into the density profile across the interface of the PE/surfactant solutions [13–16]. The role salt concentration has on aggregation and precipitation of PE and PE-surfactant solutions is also an open problem [6]. There are recent suggestions that at high salt concentrations, macromolecules may be overscreened by counterions, effectively reversing their charge [17–19], and that same-charge macromolecules may attract each other in several density regimes [20].

Previous studies on surfactant-polyelectrolyte complexes have focused on bulk properties and self-assembly as driven by surfactant concentration. The present study focuses on interfacial behavior; in particular, on the role played by the gas-water interface in the precipitation process, and how the self-assembly may be controlled by the weakening of the electrostatic interactions (salt concentration). Herein, we report surface sensitive synchrotron x-ray diffraction studies, both reflectivity and diffraction at grazing angles of incidence (GIXD) on a model system consisting of sodium dodecyl sulfate (SDS) and Poly-diallyldimethylammonium chloride (PDAC) (molecules are shown in Fig. 1). SDS ( $C_{12}H_{27}O_4SNa$ ) and PDAC ( $MW = 100\,000\text{--}200\,000$ ) [ $C_8H_{16}NCl$ ] $_n$ ;  $n =$

685–1370; obtained from Sigma-Aldrich (2002 Sigma-Aldrich catalog numbers L-4509 and 40 901-4, respectively). PDAC at 2% (by weight; concentration of PE charges was 0.137 M) in pure water (Milli-Q apparatus Millipore Corp., or Bedford, MA; resistivity, 18.2M  $\Omega$  cm) and in 0.1M NaCl was used in all experiments. After stirring for 10–20 min, solutions were poured into a temperature-controlled Teflon Langmuir trough maintained at 19 °C and enclosed in a gas tight aluminum container, where surface tension was measured with a microbalance using a Wilhelmy filter-paper plate.

Surface sensitive x-ray diffraction studies of the structure of free gas-solution interface were conducted on the Ames Laboratory Liquid Surface Diffractometer at the Advanced Photon Source (APS) beam line 6ID-B (described elsewhere [21]). The highly monochromatic beam (8 keV and 16.2 keV, or  $\lambda = 1.5498$  and 0.765 334 Å, respectively), selected by a downstream Si double crystal monochromator, is deflected onto the liquid surface to a

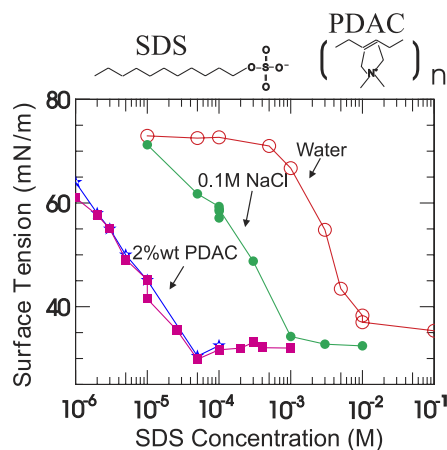


FIG. 1 (color online). Chemical structure of sodium dodecyl sulfate, SDS, and poly-diallyldimethylammonium chloride, PDAC, used in this study. Surface tension as a function of SDS concentration in water, and 0.1M NaCl and 2% PDAC both at 0 and 0.1M NaCl, practically indistinguishable.

desired angle of incidence with respect to the liquid surface by a second monochromator [Ge(111) and Ge(220) crystals at 8.0 and 16.2 keV, respectively]. Specular x-ray reflectivity experiments yield the electron density (ED) profile across the interface, and can be related to molecular arrangements in the film. The ED profile across the interface is extracted by refining a slab model that best fits the measured reflectivity by nonlinear least-squares method. The reflectivity from the slab model at a momentum transfer  $Q_z$  is calculated by  $R(Q_z) = R_0(Q_z)e^{-(Q_z\sigma)^2}$ , where  $R_0(Q_z)$  is the reflectivity from steplike functions calculated by the recursive dynamical method and  $\sigma$  is an effective surface roughness [21,22]. The GIXD measurements are performed at a fixed-angle incident beam smaller than the critical angle for total reflection from the surface, yielding the in-plane ordering within the penetration depth of the x-ray beam [21–23].

Surface tension versus SDS concentration in salt solution (0.1M NaCl) and in pure water for comparison are shown in Fig. 1, and similarly for 2% wt PDAC solutions in pure water and in 0.1M NaCl solution. The critical micelle concentration (CMC) of SDS in pure water is significantly reduced with the addition of 0.1M NaCl, a result documented in the literature [10,12,24]. The onset for the reduction in surface tension at 0.1M NaCl occurs at SDS concentrations 2 orders of magnitude lower than those of SDS in pure water [25]. Likewise, in the presence of the polyelectrolyte, Fig. 1 shows that the lowering of surface tension occurs at even lower SDS concentrations, suggestive of the formation of highly hydrophobic surfactant-polyelectrolyte complexes [11,26]. Within experimental error, our measurements in Fig. 1 show surface tension as a function of SDS concentration with 2% wt. PDAC is not affected by the addition of simple salt (NaCl 0.1M) to water. This implies the addition of salt to PDAC does not affect the total amount of excess material at the interface.

X-ray reflectivity and GIXD studies of PDAC solutions surfaces were conducted at various SDS concentrations (with and without 0.1M NaCl). Figure 2 shows a sequence of normalized reflectivities,  $R/R_F$  (where  $R_F$  is the calculated reflectivity of an ideally flat water interface) for a typical SDS concentration, ( $10^{-4}M$ ) in pure water and in PDAC solutions, and after adding 0.1M NaCl to the same solution. Up to SDS concentrations slightly higher than  $10^{-4}M$  (in pure water), the reflectivity [Fig. 2(A)] is similar to that of a pure water surface, although with a surface roughness  $\sigma = 3.5 \text{ \AA}$ , significantly larger than that measured for a water surface under similar conditions and with the same instrumental setup ( $\sigma_w \approx 2.4 \text{ \AA}$ ). The enhanced surface roughness is evidence for the presence of a dilute inhomogeneous SDS film at the air-water interface. The addition of NaCl to the SDS solution ( $10^{-4}M$ ) modifies the reflectivity, giving rise to a minimum at  $Q_z \approx 0.53 \text{ \AA}^{-1}$ , due to the formation of a

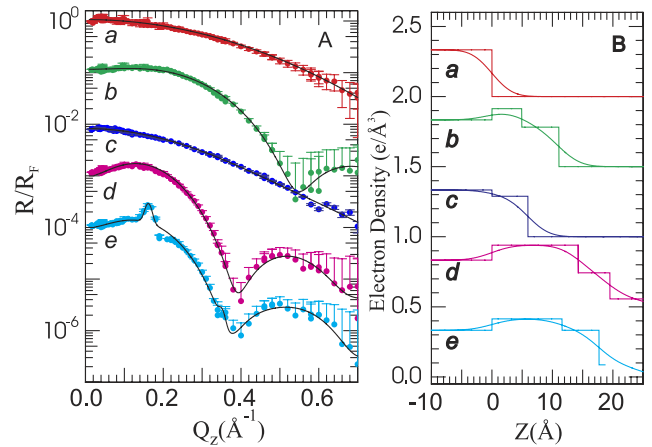


FIG. 2 (color online). (A) Reflectivity normalized to  $R_F$  ( $R_F$  is the reflectivity from ideally flat water interface) for (a)  $10^{-4}M$  SDS in water, (b)  $10^{-4}M$  SDS 0.1M NaCl, (c) 2% wt PDAC in pure water, (d)  $10^{-4}M$  SDS in 2% wt PDAC solution, (e)  $10^{-4}M$  SDS 2% wt PDAC after the addition of 0.1M NaCl. (Reflectivities are shifted by a decade for clarity.) (B) Electron density profiles ( $Z = 0$  is the molecule-solution interface) used to generate the fitted reflectivity [solid lines in (A)], the steplike functions (box model) are generated assuming no surface roughness ( $\sigma = 0$ ; ED's are shifted for clarity).

more homogeneous film. The detailed analysis in terms of a two-box model [22] yields the ED profile shown in Fig. 2(B) with a total film thickness  $d_{\text{total}} = 12 \text{ \AA}$ , compared to the estimated stretched SDS molecule  $d_{\text{st}} = 19.3 \text{ \AA}$ . This implies abundant *gauche* defects and/or a large average molecular tilt angle with respect to the surface normal [ $t = \text{acos}(d_{\text{total}}/d_{\text{st}})$ ]. Additional reflectivity studies as a function of SDS concentrations (with and without NaCl) show a systematic increase of total film thickness, up to  $\approx 18 \text{ \AA}$ , with the increase of SDS concentration [27]. Assuming an average SDS molecular area  $A$ , the number of electrons per SDS molecule (including adsorbed molecules— $\text{H}_2\text{O}$  or ions)  $N_{\text{ref}}$  is given by

$$N_{\text{ref}} = N_{\text{SDS}} + N_{\text{other}} = A \int \rho(z) dz, \quad (1)$$

where  $N_{\text{SDS}} = 148$  electrons and  $N_{\text{other}}$  is the number of electrons due to integrated water molecules or ions inseparable from the topmost layer. Using Eq. (1) and the ED profiles, the lower limit for the SDS molecular area (i.e.,  $N_{\text{other}} = 0$ ), is  $A_{\text{min}} \approx 35.6 \text{ \AA}^2$ , whereas assuming two bound water molecules per SDS molecule yields  $A \approx 40.4 \text{ \AA}^2$ , in agreement with values extracted from surface tension isotherms [24]. The reflectivity from 2% PDAC solution (no SDS) shown in Fig. 2(A) demonstrates that the effect of pure PE on the surface, even at this high concentration, is negligible. The addition of SDS to 2% PDAC solution brings the minimum in  $R/R_F$  to  $Q_z \approx 0.38 \text{ \AA}^{-1}$ , showing the film is thicker ( $d_{\text{total}} \approx 22.5 \text{ \AA}$ )

and more organized than that of SDS in water or salt solution. The head-group region is significantly thicker than that of SDS solutions ( $d_{\text{head}} \approx 11 \text{ \AA}$ ), suggesting the interfacial film consists of a PDAC-SDS complex. The ED and thickness of the topmost slab indicate the hydrocarbon tails are loosely packed as in a 2D liquid state. The most dramatic effect in the reflectivity is observed with the addition of salt to the PDAC-SDS solution, where Bragg reflections are superimposed on the reflectivity at  $Q_z^I \approx 0.165 \text{ \AA}^{-1}$  and at  $Q_z^{II} \approx 0.345 \text{ \AA}^{-1}$ . These two peaks, as shown below, are the first and second order Bragg reflections from hexagonal structures due to closely-packed cylindrical micelles with their long axis parallel to the liquid surface. Similar neutron reflectivity studies of the dilute PDAC solutions with SDS and NaCl are consistent with the present findings [16,28].

The picture of a liquidlike film with disordered SDS at the gas-water interface is validated by our GIXD studies. Figure 3(A) shows diffraction patterns (wide-angle) of pure water surface [29], and that of the PDAC-SDS ( $2 \times 10^{-4} M$ ). The difference between the two patterns at two SDS concentrations is shown in Fig. 3(B). The broad peak in the diffraction at  $Q_r = 1.34 \text{ \AA}^{-1}$  of an average  $4.69 \text{ \AA}$   $d$  spacing is due to scattering from 2D-liquid hydrocarbon chains (typical  $d$  spacing for hexagonally ordered hydrocarbon chains is  $4.2 \text{ \AA}$ ). The linewidth of the peak,  $\Delta Q = 0.31 \text{ \AA}^{-1}$ , with average correlation length  $\xi \approx 20 \text{ \AA}$ , is further evidence for the 2D disordered chains [30]. At small angles, the GIXD reveals several discrete Bragg reflections of a diffraction pattern from crystals highly oriented with respect to the water surface. These reflections are related to those observed in the reflectivity. As shown in Fig. 4(A) and 4(B), these peaks are sharp, characteristic of 3D ordering, with no rodlike scattering typical of a quasi-2D system. The positions of the peaks observed and their layout as shown in Fig. 4(C)

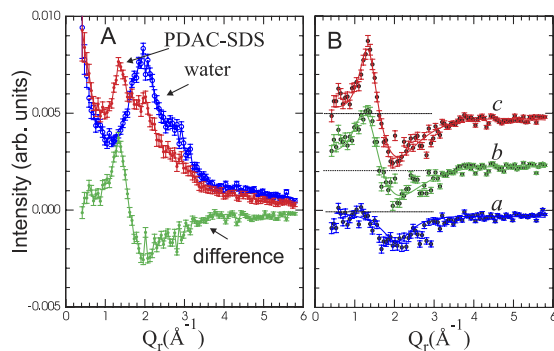


FIG. 3 (color online). (A) In-plane diffraction (GIXD) scans of pure water, and 2% wt PDAC  $2 \times 10^{-5} M$  SDS and  $0.1 M$  NaCl as indicated and the difference between the two scans. (B) Similar differences between solutions of 2% wt PDAC (a)  $0 M$  SDS, (b)  $2 \times 10^{-5} M$  SDS, (c)  $2 \times 10^{-4} M$  SDS (scans shifted for clarity). The disruption of the structure of water at the interface is apparent.

are consistent with a slightly distorted hexagonal structure, as depicted in Fig. 4(D) with  $a = 40.3 \pm 0.5 \text{ \AA}$ ,  $b = 44.6 \pm 0.6 \text{ \AA}$ , and  $\gamma = 121 \pm 1 \text{ deg}$ . The peaks observed are similar, although not the same, as those observed by Chu and coworkers [1,2] in small angle x-ray scattering experiments from related systems. Based on the anisotropy observed, we propose a simple structure of stacked cylindrical micelles with their long axis parallel to the water surface, forming a 2D polycrystalline system with preferred orientation with respect to the surface.

The distorted hexagonal diffraction pattern indicates the growth is anisotropic and implies the interface plays a role in initiating complexation (aggregation) processes. Another important result is the effect the addition of salt (NaCl) has on promoting PE/surfactant crystallization. Our heuristic interpretation of the aggregation and subsequent crystallization is depicted in Fig. 5. The PE, with no surfactants or salt added, is highly soluble in water and is repelled from the air-water interface, due to the discontinuity in dielectric constant [31]. A minute increase in surfactant concentration lowers surface tension (see Fig. 1) and initiates the micellization. We argue that micelle formation is initiated at the interface as the ideal linear bulk separation among surfactants is  $\approx 250 \text{ \AA}$  [surfactant concentrations ( $\approx 10^{-4} M$ )], and that the addition of NaCl to the PE/surfactant solution screens electrostatic interactions, leading to cylindrical micelles [25]. Absorption of PE to micelles is then expected to be enhanced by the mechanism of counterion release [32]. We speculate that micelles will then self-attract by a similar correlation mechanism, as recently observed in multivalent ions [33], eventually condensing into a hexagonal (columnar) crystal, and thus growing crystals from the interface. In

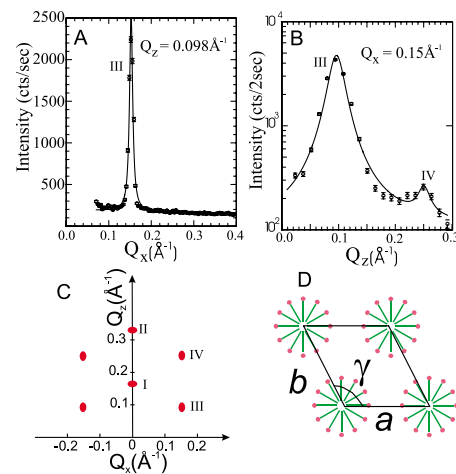


FIG. 4 (color online). (A) A scan along  $Q_x$  of (10) peak at  $Q_z = 0.098 \text{ \AA}^{-1}$ . (B) A rod scan along the same peak (logarithmic scale) also revealing the (11) peak. (C) The observed peaks in the  $Q_x, Q_z$  plane. (D) A schematic illustration of the suggested model structure with the oblique unit cell. The long axes of cylindrical micelles are parallel to the liquid surface.

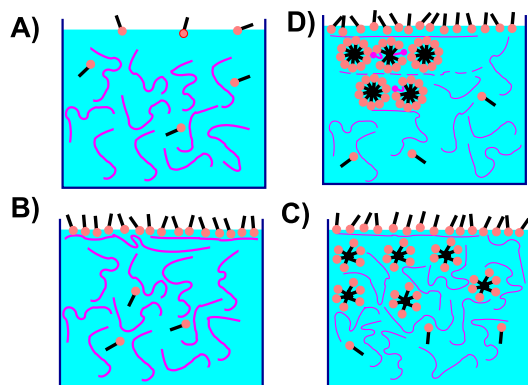


FIG. 5 (color online). (A) Schematic pathways of complexation and subsequent crystallization. (A) Negligible surfactant concentration—the PE is repelled from the interface. (B) Below the CAC a PE surfactant is formed at the interface. (C) Critical aggregation concentration (CAC) is reached and micellization occurs. (D) The addition of salt transforms micelles to cylindrical shape and crystallizes them. The arrangement and location of the PE in the crystalline regions (shown with a dashed line) was not be determined in this study.

summary, we have shown the fundamental role played by the interface in nucleating PE-surfactant complexes and how crystallization may be induced by salt concentration at minute surfactant concentrations. The location of the PE and the ions in this crystallization process is not known, but we hope that the application of anomalous x-ray reflectivity and GIXD techniques utilizing heavier ions [34] (CsCl as a salt, for instance) will provide a more detailed internal structure of the crystals.

We wish to thank M. Muthukumar and D. S. Robinson for helpful discussions. The MUCAT sector at the APS is supported by the U.S. DOE Basic Energy Sciences, Office of Science, through Ames Laboratory under Contract No. W-7405-Eng-82. Measurements were supported by the U.S. DOE, Basic Energy Sciences, Office of Science, under Contract No. W-31-109-Eng-38.

- [1] B. Chu *et al.*, *Macromolecules* **28**, 8447 (1995).  
 [2] F. Yeh *et al.*, *J. Am. Chem. Soc.* **118**, 6615 (1996).  
 [3] P. Hanson, *Langmuir* **14**, 4059 (1998).  
 [4] K. Kogej *et al.*, *Langmuir* **17**, 3175 (2001).  
 [5] P. Hanson, *Langmuir* **17**, 4167 (2001).  
 [6] M. J. Leonard and H. H. Strey, *Macromolecules* **36**, 9549 (2003).  
 [7] J.-F. Berret *et al.*, *Macromolecules* **37**, 4922 (2004).  
 [8] I. Koltover *et al.*, *Science* **281**, 78 (1998); Strey *et al.*, *Curr. Opin. Struct. Biol.* **8**, 309 (1998).  
 [9] G. C. L. Wong *et al.*, *Science* **288**, 2035 (2000).

- [10] M. J. Rosen, *Surfactants and Interfacial Phenomena* (Wiley, New York, 1978).  
 [11] *Interactions of Surfactants with Polymers and Proteins*, edited by E. D. Goddard and K. P. Ananthapadmanabham (CRC Press, Boca Raton, 1993).  
 [12] P. C. Hiemenz and R. Rajagopalan, *Principles of Colloid and Surface Chemistry* (Marcel Dekker, Inc., New York, 1997).  
 [13] J. R. Lu *et al.*, *J. Colloid Interface Sci.* **174**, 441 (1995).  
 [14] C. Stubenrauch *et al.*, *Langmuir* **16**, 3206 (2000).  
 [15] H. Yim *et al.*, *Macromolecules* **33**, 6126 (2000).  
 [16] E. Staples *et al.*, *Langmuir* **18**, 5139 (2002).  
 [17] J. F. Joanny, *Eur. Phys. J. B* **9**, 117 (1999).  
 [18] T. T. Nguyen, A. Yu. Grosberg, and B. I. Shklovskii, *J. Chem. Phys.* **113**, 1110 (2000).  
 [19] A. D. Dobrynin, A. Deshkovski, and M. Rubinstein, *Macromolecules* **34**, 3421 (2001).  
 [20] W. M. Gelbart, R. F. Bruinsma, P. A. Pincus, and V. A. Parsegian, *Physics Today* **53**, No. 9, 38 (2000).  
 [21] D. Vaknin, in *Methods in Materials Research*, edited by E. N. Kaufmann *et al.* (Wiley, New York, 2001), p. 10d.2.1.  
 [22] J. Als-Nielsen and K. Kjaer, *NATO ASI Ser. B*, **211**, 113 (1989).  
 [23] The coordinates of the momentum transfer ( $Q_x$ ,  $Q_y$ ,  $Q_z$ ) are such that  $Q_x$  is normal to the scattering plane at specular-reflectivity configuration,  $Q_y$  is parallel to the surface and in the scattering plane, and  $Q_z$  is normal to the liquid surface.  
 [24] A. J. Prosser and E. I. Franses, *Colloids Surf. A* **178**, 1 (2001).  
 [25] C. Tanford, *The Hydrophobic Effect: Formation of Micelles and Biological Membranes* (John Wiley and Sons, New York, 1980).  
 [26] T. Wallin and P. Linse, *Langmuir* **14**, 2940 (1998); C. Von Ferber and H. Lowen, *J. Chem. Phys.* **118**, 10774 (2003).  
 [27] D. Vaknin (to be published).  
 [28] J. Penfold *et al.*, *Langmuir* **20**, 2265 (2004).  
 [29] For bulk water the first peak in the structure factor is observed at  $Q_r \approx 2.0 \text{ \AA}^{-1}$  compared to the  $1.96 \text{ \AA}^{-1}$  as measured with GIXD evanescent x-ray wave with main contribution to the structure factor from the top most water layers. The shift in the position of the first peak indicates a slightly larger O-O  $d$  spacing at the interface.  
 [30] The first and strongest peak, in the structure factor of liquid alkanes is found at the  $1.3\text{--}1.4 \text{ \AA}^{-1}$ ; see, e.g., A. Habenschuss and A. H. Narten, *J. Chem. Phys.* **92**, 5692 (1990).  
 [31] W. K. H. Panofsky and M. Philipis, *Classical Electricity and Magnetism* (Addison-Wesley, Reading, MA 1972).  
 [32] R. Bruinsma, *Eur. Phys. J. B* **4**, 75 (1998).  
 [33] Angelini *et al.*, *Proc. Natl. Acad. Sci. U.S.A.* **100**, 8634 (2003).  
 [34] D. Vaknin, P. Kruger, and M. Lösche, *Phys. Rev. Lett.* **90**, 178102 (2003).